Nanocellulose from citrus processing waste using water and electricity only

Samar Al Jitan
Khalifa University of Science and Technology
Antonino Scurria
Istituto per lo Studio dei Materiali Nanostrutturati, CNR https://orcid.org/0000-0001-5624-6833
Lorenzo Albanese
Istituto per la Bioeconomia, CNR https://orcid.org/0000-0002-4549-8514
Mario Pagliaro
Istituto per lo Studio dei Materiali Nanostrutturati, CNR https://orcid.org/0000-0002-5096-329X
Francesco Meneguzzo
Istituto per la Bioeconomia, CNR https://orcid.org/0000-0002-5952-9166
Federica Zabini
Istituto per la Bioeconomia, CNR https://orcid.org/0000-0003-1505-0839
Reem Al Sakkaf
Khalifa University of Science and Technology
Ahmed Yusuf
Khalifa University of Science and Technology
Giovanni Palmisano (giovanni.palmisano@ku.ac.ae)
Khalifa University of Science and Technology https://orcid.org/0000-0001-9838-6252
Rosaria Ciriminna (rosaria.ciriminna@cnr.it)
Istituto per lo Studio dei Materiali Nanostrutturati, CNR https://orcid.org/0000-0001-6596-1572

Short Report

Keywords: Nanocellulose, Hydrodynamic cavitation, Citrus processing waste, Cellulose nanofiber, CytroCell

Posted Date: May 17th, 2021

DOI: https://doi.org/10.21203/rs.3.rs-534535/v1

Abstract

Along with a water-soluble fraction rich in pectin, the hydrodynamic cavitation of citrus processing waste carried out in water directly on a semi-industrial scale affords an insoluble fraction consisting of a new nanocellulose of high quality. Lemon and grapefruit nanocellulose powders isolated upon filtration and mild drying consist, respectively, of 100-500 nm wide cellulose nanorods, and of 500-1,000 nm wide ramified microfibrils extending for several μm. The process is general and can be applied to any citrus processing biowaste. These findings establish a long-sought technically viable route to a material whose numerous potential applications in fields ranging from biomedicine to composite production have been limited by the harsh conditions required for the extraction of nanocellulose via acid or enzymatic hydrolysis following pretreatment of lignocellulosic biomass with acid-chlorite or alkali.

1. Introduction

Termed “ageless bionanomaterial” by Dufresne,[1] nanocellulose is a nanoscale material consisting either of cellulose nanocrystals (CNC, also called nanocrystalline cellulose) or cellulose nanofibrils (CNF, also called nanofibrillated cellulose) having exceptional chemical, mechanical, biological, optical and thermal properties.[2] Potential applications range from transparent and foldable material in flexible energy and electronic devices,[3] through carmaking using nanocellulose-reinforced polymer composites.[4] Being biocompatible, chemically stable and hydrophilic, nanocellulose also has numerous potential biomedical new usages.[5]

Large-scale production of this versatile biomaterial so far has been limited by the demanding physical and chemical conditions, required first to separate the lignin from wood lignocellulosic biomass, and then to extract nanocellulose from the latter cellulosic fraction.[1,2] Following the separation step using either acid-chlorite or alkaline treatment (and thus generating large amounts of wastewater), nanocellulose is generally extracted via acid hydrolysis (adding to the wastewater burden), steam explosion (with high energy consumption), enzymatically (requiring overly long extraction times), mechanically (high pressure homogenization, and ball milling methods) or by ultrasonication, with large energy demand.[2]

Comprised of cellulose I only, CNC has a low aspect ratio (length/diameter = 10-100), a tensile strength similar to that of aramid-fiber (10 GPa), and is produced via acidic hydrolysis of plant (wood, cotton, etc.) cellulose pulp. Its suspensions have liquid-crystalline properties. CNF has a high aspect ratio (length/diameter = 100-150), includes amorphous cellulose along with cellulose I, and is produced via mechanical processes. Its dispersions in water exhibit gel-like characteristics.

The industrial production of CNC from wood cellulose pulp using sulphuric acid has an estimated production cost ranging from $3632/t to $4420/t, with feedstock cost and capital investment being the major cost drivers.[6] Yet, in the same year of these estimates (2017) for large scale production, CNC was reported to be sold at $1,000/kg.[7]

In 1998, Isogai and Sato successfully applied the polysaccharide selective oxidation process discovered by de Nooy to regenerated and mercerized cellulose[8] in order to partly convert the primary alcohol groups of cellulose to carboxylates using catalytic amounts of 2,2,6,6-tetramethylpiperidine-1-oxyl (TEMPO) and sodium bromide with aqueous NaOCl as primary oxidant.[9] Eight years later, the team in collaboration with Vignon discovered that native celluloses could be fibrillated in 3-5 nm nanofibrils by simple mechanical homogenization of the solution containing the TEMPO-oxidized cellulose.[10] The electrostatic repulsions between the cellulose fibrils bearing the carboxylate groups cause the shear and dispersion of the nanofibrils under mechanical agitation.

Since 2017, the process is used by a large paper company in Japan to manufacture CNF in the form of nano-dispersed fibers with uniform fiber width of 3 to 4 nm starting from bleached wood pulp at two different paper mills.[11] The company supplies the 'Cellenpia' product series using CNF as key ingredient to different industrial customers producing CNF-reinforced tires, paper barrier cups for beverages, personal care, hygiene, and cosmetic products. In 2019, the same company successfully developed a CNF-reinforced resin that was used to produce a demonstration car (the Nano Cellulose Vehicle)[12] whose weight compared to a conventional car was reduced by around 10%.

Today, CNF is sold at a cost of $90-100/kg.[13] This high cost is due both to the high cost of TEMPO as well as of processing the spent hypochlorite dilute solution containing the TEMPO catalyst. Separating nitroxyl radicals in solution is a multi-step, expensive process.[14] Furthermore, TEMPO is a genotoxic ingredient[15] whose concentration in any material suitable for biomedical use, must be lower than a low threshold of toxicological concern (*i.e.*, 4 ppm).[16]

In order to lower production costs, cellulose feedstocks alternative to wood pulp have been widely explored. Available in over 100 million tonne yearly amount, waste orange peel - namely the main citrus processing waste (CPW) obtained from the orange juice processing industry - would be an ideal feedstock. Unfortunately, the routes to citrus nanocellulose starting from CPW based on enzymatic,[17] microwave-assisted hydrothermal treatment,[18] and acid hydrolysis,[19] all present significant technical limitations.

For example, the nanocellulose fibrils obtained via multi-step microwave-assisted extraction of dried depectinated orange peel are deeply colored in brown due both to caramelized sugars and to the Maillard reaction between sugars and residual proteins at the high working temperatures required for extraction (120 °C to 180 °C).[18]

Now, we report that the insoluble fraction resulting from the hydrodynamic cavitation (HC) of citrus processing biowaste carried out on a semi-industrial scale in water consists of a new nanocellulose of high quality. Dubbed "CytroCell",[20] this citrus nanocellulose is readily obtained in large amounts through a one-pot process requiring no prior or subsequent chemical or mechanical treatment.

2. Experimental

Obtained as described elsewhere[21,22] by processing in 120 L >30 kg of citrus (lemon or grapefruit) industrial processing waste from fruits organically grown in Sicily, the CytroCell samples were simply isolated by filtration of the aqueous suspension resulting from the HC-assisted extraction. After filtration, the solid CytroCell residue was mildly dried in an oven at 40 °C. Samples consisting of yellow (in the case of lemon) or pink (in the case of grapefruit) CytroCell with a delicate citrus scent were readily isolated. No further treatment was necessary beyond manual removal of a few lignin particles visually identified amid the CytroCell fibers in a glass Petri dish.

The transmission electron microscopy (TEM) analysis was performed by using a Tecnai G2 microscope operating at 200 kV. The TEM sample was prepared by suspending a very small amount of cellulose sample in deionized water, treating with ultrasounds, and finally depositing 5 µL of the diluted suspension on a 400-mesh Cu grid provided by Ted Pella (Redding, CA, USA). The solvent was evaporated at room temperature overnight. ImageJ image processing open source program was used for the analysis of the sample dimensions.

The X-ray diffraction (XRD) measurements were carried out using a XRD PANalytical Empyrean diffractometer, with a Cu *K*α radiation of 1.54 Å, a scan step-size of 0.0167° and a 2θ scan range of 5-40°. The thermogravimetric and differential thermal analyses (TGA/DTA) were performed using a Netzsch STA 449 F3 Jupiter thermal analyzer (NETZSCH-Gerätebau, Selb, Germany) using samples of ca. 13 mg. The temperature was increased from 25°C to 700°C at a constant heating rate of 10°C/min under N_2 flow.

The zeta potential was measured with a Zetasizer Nano ZS analyzer (Malvern Panalytical, Malvern, Great Britain) using a laser wavelength of 633 nm. Measurements carried out in a DTS1070 cell on a suspension of CytroCell (10 mg) in 1 L ultrapure (milli-Q) obtained using a Smart2Pure water purification system (Thermo Fisher Scientific, Waltham, MA, USA) water. The pH of the suspension was adjusted using 0.3 M HCl and 0.5 M NaOH.

Adsorption-desorption isotherms were determined using the a NOVA 2000e surface area and pore size analyzer (Quantachrome, Boynton Beach, FL, USA) with cryogenic N_2 as adsorbate. The CytroCell samples were first degassed under vacuum at about 110 °C overnight. The specific surface area of samples was determined using the multipoint Brunauer-Emmett-Teller (BET) model, using the average adsorption and desorption values of P/P_o in the range 0-0.35. The pore size distribution was calculated using the adsorption curve for all ranges of P/P_o by using the Barrett-Joyner-Halenda (BJH) model.

A Quanta 250 FEG scanning electron microscope (SEM) equipped with ETD detector (Thermo Fisher Scientific, Waltham, MA, USA) was used to study the morphology of the cellulose samples. A small fragment of each sample was deposited on a carbon tape attached to the stainless-steel stub to be loaded into the SEM using the stub holder. Each sample was sputter-coated with a thin layer (~10 nm) of gold as a conductive material to enhance the quality of the resulting images.

3. Results And Discussion

Figure 1 displays the TEM images of lemon CytroCell at two different degrees of magnification. The material is comprised of cellulose 0.5-3 mm long microfibrils whose section varies between about 110 and 420 nm (Figure 1, bottom). The TEM photographs for grapefruit CytroCell in Figure 2 display a different nanostructure consisting of ramified microfibrils whose diameter varies from 500 nm to 1 μm. Although this sample is mainly composed of cellulose microfibers, some residual amorphous matter (lignin) was detected from the TEM image at higher magnification (red arrows in bottom of Figure 2).

Repeated at Khalifa University of Science and Technology, the XRD measurements (plots not shown) confirmed previous XRD analysis showing that both CytroCell materials consist of cellulose of low crystallinity index (0.33 for lemon and 0.36 for grapefruit CytroCell).[20] Again, the grapefruit-derived cellulose was found to contain more abundant calcium oxalate crystals (with diffraction peaks at about 14.6°, 24.4° and 29.3°), abundant in both the lemon and grapefruit fruit peel,[23] and particularly abundant in plants grown in dry climates such as that of southern Sicily where both citrus fruits used to produce CytroCell originate (under drought conditions oxalate releases CO_2 and water molecules).[24]

The SEM images of both lemon abd grapefruit CytroCell in Figure 3 show a compact and relatively convoluted surface for both lemon nanocellulose nanorods and grapefruit nanocellulose microfibrils. These are the surfaces interacting with probe molecules such as the N_2 molecules during the surface area and pore size cryogenic measurements, or with the H_2O molecules when immersed in water. We briefly remind that these nanocelluloses adsorb and retain 8 g_{water}/g_{cell} in the case of lemon CytroCell and 5 g_{water}/g_{cell} for grapefruit CytroCell.[20] In general, for powdered an dhighly purified wood cellulose used as dietary fiber, the WHC increases with increasing fiber length.[25]

The fact that the water holding capacity (WHC) of lemon nanocellulose of significantly shorter fiber length is higher than that of grapefruit nanocellulose suggests a different chemical composition of lemon CytroCell nanocellulose.

Based on the IR analysis, this difference has been ascribed to the partial esterification of lemon CytroCell and the primary alcohol groups with citric acid residual in the wet lemon processing biowaste during the HC-assisted extraction.[20] Highly hydrophilic free and esterified carboxyl groups of the esterified cellulose enhance the WHC.

The difference in the amount of water adsorbed in the materials as such is noted also in the thermogravimetric analysis/differential scanning analysis (TGA/DTA) profiles of the two materials displayed in Figure 4.

The first weight loss around 100 °C corresponding to evaporation of bonded water in cellulose is higher for lemon CytroCell, whereas the onset of thermal degradation at 42 °C occurs 5 °C ahead of that for grapefruit nanocellulose (47 °C). The TGA and DTA profiles until the maximum degradation temperature

(340 °C for lemon and 337 °C for grapefruit) are very similar, with two peaks, one near 240 °C and another near 340 °C. Based on recent thermal stability analysis of different nanocelluloses,[26] the first peak is ascribed to the decomposition of negatively charged carboxyl groups on the fibril surfaces (introduced by reaction with residual citric acid), whereas the second is assigned to pyrolysis of cellulose.

The higher amount of carboxylate groups in lemon-derived CytroCell (visible in the IR spectra)[20] is reflected in the additional weight loss slope variation in the TGA and peak in the DTA profile for the lemon-derived nanocellulose at around 500 °C, which likely corresponds to the decomposition of the glycosyl-units resulting from the previous decomposition of the citric acid-esterified groups, followed by the formation of a carbonaceous residue.

Using a different porosimeter (Quantachrome NOVA 2000e) equipped with different burette when compared to that using the Micromeritics ASAP 2020 Plus used in previous surface area and pore size measurements, we were able to measure the adsorption-desorption isotherms of the free (*i.e.* non-aggregated powder) samples as originally reported,[20] when due to the high electrostatic charge on the surface of both nanocelluloses we could solely use an aggregate rather than a powdered specimen to carry out the N_2 adsorption and desorption experiments.

The new adsorption experiments using the free powders returned a very similar pore size of 1.64 nm and 1.69 nm for lemon and grapefruit CytroCell, confirming that these new celluloses are mesoporous materials. The corresponding 24 and 27 nm pore sizes previously reported for the aggregate material,[20] describe the porosity of nanocellulose aggregates.

The zeta potential of lemon CytroCell at neutral pH measured several months after storage at room temperature under regular atmosphere, was slightly lower (-25 mV) that that measured for the freshly obtained sample (-29.5 mV) whereas that of grapefruit CytroCell (-32 mV) was significantly larger than that of freshly obtained (-22.67 mV).[20] What is further relevant in light of forthcoming practical applications is that the zeta potential varies at relatively slow pace in a wide range of pH values comprised between pH 4 and 13 (Figure 5), starting to change at a higher rate only at and below pH 3.

This behavior is similar to that of nanocellulose obtained in the form of CNC upon hydrolysis of wood pulp with sulphuric acid.[27] In the latter case, varying the pH across a wide range from pH 2 to pH 10 had little effect on CNC zeta potential until pH 1, when complete protonation of the sulphate groups is observed. In the present case, complete protonation of the bound citrate groups occurs at about pH 2.0 for both nanocelluloses with a significant decrease of the zeta potential noted at pH 4 for both citrus nanocelluloses.

The experimental zeta potential values showed large standard deviation values, particularly at neutral and alkaline pH. These large variations may be due to fibrillar structure of both CNF samples made progressively less stable by the addition of both base.

The zero charge point at pH 2.0 due to neutralization of the negative charge of the free carboxylate citrate groups by protons, for both lemon and grapefruit samples depends on the pK_a of the bound citrate groups. This finding, likewise to what happens for bound sulphate groups for CNC extracted with H_2SO_4,[27] confirms that the carboxylate groups bound to the surface of both citrus nanocelluloses originate from citrate groups.

4. Conclusions

In conclusion, along with a water-soluble fraction rich in pectin functionalized with adsorbed flavonoids and terpenes, the hydrodynamic cavitation of citrus processing waste in water affords an insoluble fraction consisting of a new nanocellulose of high quality.

Directly carried out on a semi-industrial scale (>30 kg citrus biowaste in 120 L water), this cellulosic material is readily obtained in large amounts through an efficient, one-pot process requiring no chemical reactant. Water is the only dispersion medium, and electricity is the unique energy form employed to run the cavitation process affording plentiful amounts of a material whose numerous potential applications so far have been limited by multistep production processes requiring harsh conditions.[1,2]

The TEM analysis shows that lemon CytroCell nanocellulose consists of 100-500 nm wide cellulose nanorods, whereas grapefruit nanocellulose is comprised of 500-1,000 nm wide ramified microfibrils extending for several µm. Both materials are mesoporous with pore size approaching 1.7 nm.

Here demonstrated for lemon and grapefruit processing waste, the process is general and can be applied to any citrus processing biowaste including that resulting from orange juice production.[28]

Theses findings establish a long-sought technically viable direct route to citrus-derived nanocellulose using water and electricity only. No toxic or harmful effluents are generated during the extraction process, thereby dramatically reducing the operating expenses when compared to conventional extraction routes based on lignocellulosic biomass pretreatment with acid-chlorite or alkali followed by extraction of nanocellulose via acid or enzymatic hydrolysis.[2] The safe and robust hydrodynamic cavitation process for the extraction of natural products is easily scaled-up.[29] Forthcoming studies will shotly demonstrate the technical and economic viability of upscaling the process to convert citrus biowaste into highly valued nanocellulose and pectin bioproducts via controlled hydrodynamic cavitation.

Declarations

Acknowledgments

Thanks to OPAC Campisi (Siracusa, Italy) for kindly providing the lemon and grapefruit processing waste from which the lemon and grapefruit cellulosic materials were obtained. Dr. Cyril Aubry is gratefully acknowledges for his assistance during the characterization at the electron microscopes.

Conflict of interest

The Authors declare no conflict of interest.

Funding

No specific funding was used for this research. The Authors used internal resources available in their respective laboratories.

References

1. Dufresne, Nanocellulose: a new ageless bionanomaterial, Mater. Today **2012**, 16, 220-227. doi:10.1016/j.mattod.2013.06.004
2. Phanthong, P. Reubroycharoen, X. Hao, G. Xu, A. Abudula, G. Guan, Nanocellulose: extraction and application, *Carbon Resour. Convers.* **2018**, *1*, 32-43. doi:10.1016/j.crcon.2018.05.004
3. A. Titton Dias, S. Konar, A. Lopes Leão, W. Yang, J. Tjong, M. Sain, Current state of applications of nanocellulose in flexible energy and electronic devices, *Front. Chem.* **2020**, *8*, 420. doi:10.3389/fchem.2020.00420
4. Adekomaya, Adaption of green composite in automotive part replacements: discussions on material modification and future patronage, *Environ. Sci. Pollut. Res*. **2020**, *27*, 8807-8813. doi: 10.1007/s11356-019-07557-x
5. Jorfi, E.J. Foster, Recent advances in nanocellulose for biomedical applications. *J. Appl. Polym. Sci.* **2015**, **132**, 41719. doi: 10.1002/app.41719
6. Abbati de Assis, C. Houtman, R. Phillips, E.M. Bilek, O. J. Rojas, L. Pal, M. S. Peresin, H. Jameel, R. Gonzalez, Conversion economics of forest biomaterials: risk and financial analysis of CNC manufacturing, *Biofuels, Bioprod. Bioref.* **2017**, *11*, 682-700. doi: 10.1002/bbb
7. Sithole, Roadmap towards innovation-driven forestry manufacturing, Biorefinery Industry Development Facility, Durban, South Africa, 4 October 2017.http://www.safcol.co.za/wp-content/uploads/2017/10/8Dr-Bruce-Sithole.ppt (accessed, May 13, 2021).
8. Isogai, Y. Kato, Preparation of polyuronic acid from cellulose by TEMPO-mediated oxidation, *Cellulose* **1998**, *4*, 153-164. doi:10.1023/A:1009208603673
9. E. de Nooy, A. C. Besemer, H. van Bekkum, Highly selective nitroxyl radical-mediated oxidation of primary alcohol groups in water-soluble glucans, *Carbohydr. Res.* **1995**, *269*, 89-98. doi:10.1016/0008-6215(94)00343-E
10. Saito, Y. Nishiyama, J.-L. Putaux, M. Vignon, A. Isogai, Homogeneous Suspensions of individualized microfibrils from TEMPO-catalyzed Oxidation of native cellulose, *Biomacromolecules* **2006**, *7*, 1687-1691. doi:10.1021/bm060154s
11. Nippon Paper Group, Cellulose nanofiber manufacturing technology and application development , 2021. https://www.nipponpapergroup.com/english/research/organize/cnf.html (accessed, May 13,

2021).

12. Research Institute for Sustainable Humanosphere, Nano cellulose vehicle project, 2019. http://www.rish.kyoto-u.ac.jp/ncv/ (accessed, May 13, 2021).
13. Pagliaro, Cellulose nanofiber: An advanced biomaterial soon to become ubiquitous, *Chim. Oggi* **2018**, *36* (4), 61-62.
14. Jetten, A. Besemer, Process for the recovery of nitroxy compounds from organic solutions and oxidation process, US20050154206A1, (2005).
15. Szekely, M. C. Amores de Sousa, M. Gil, F. Castelo Ferreira, W. Heggie, Genotoxic impurities in pharmaceutical manufacturing: sources, regulations, and mitigation, *Chem. Rev.* **2015**, *115*, 8182-8229. doi: 10.1021/cr300095f
16. E. Strohmeyer, G. W. Sluggett, Determination and control of TEMPO, a potentially genotoxic free radical reagent used in the synthesis of filibuvir, *J. Pharm. Biomed.* **2012**, *62*, 216-219. doi:10.1016/j.jpba.2011.12.036
17. Mariño, L.L. Da Silva, N. Durán, L. Tasic, Enhanced Materials from Nature: Nanocellulose from Citrus Waste, *Molecules* **2015**, *20*, 5908-5923. doi:10.3390/molecules20045908
18. M. De Melo, J.H. Clark, A.S. Matharu, The Hy-MASS concept: hydrothermal microwave assisted selective scissoring of cellulose for in situ production of (meso)porous nanocellulose fibrils and crystals. *Green Chem.* **2017**, *19*, 3408-3417. doi:10.1039/c7gc01378g
19. Naz, N. Ahmad, J. Akhtar, N.M. Ahmad, A. Ali, M. Zia, Management of citrus waste by switching in the production of nanocellulose. *IET Nanobiotechnol.* **2016**, *10*, 395-399. doi:10.1049/iet-nbt.2015.0116
20. Scurria, L. Albanese, M. Pagliaro, F. Zabini, F. Giordano, F. Meneguzzo, R. Ciriminna, CytroCell: valued cellulose from citrus processing waste, *Molecules* **2021**, *26*, 596. doi:10.3390/molecules26030596
21. Nuzzo, L. Cristaldi, M. Sciortino, L. Albanese, A. Scurria, F. Zabini, C. Lino, M. Pagliaro, F. Meneguzzo, M. Di Carlo, R. Ciriminna, Exceptional antioxidant, non-cytotoxic activity of integral lemon pectin from hydrodynamic cavitation, *ChemistrySelect* **2020**, *5*, 5066-5071. doi:10.1002/slct.202000375.
22. Presentato, E. Piacenza, A. Scurria, L. Albanese, F. Zabini, F. Meneguzzo, D. Nuzzo, M. Pagliaro, D.F. Chillura Martino, R. Alduina, R. Ciriminna, A new water-soluble bactericidal agent for the treatment of infections caused by Gram-positive and Gram-negative bacterial strains, *Antibiotics* **2020**, *9*, 586. doi:10.3390/antibiotics9090586
23. L. Clements, Organic Acids in Citrus Fruits. I. Varietal Differences, *J. Food Sci.* **1964**, *29*, 276-280. doi:10.1111/j.1365-2621.1964.tb01731.x
24. Karabourniotis, H.T. Horner, P. Bresta, D. Nikolopoulos, G. Liakopoulos, New insights into the functions of carbon–calcium inclusions in plants, *New Phytol.* **2020**, 228, 845-854. doi:10.1111/nph.16763
25. F. Ang, Water Retention Capacity and Viscosity Effect of Powdered Cellulose, *J. Food Sci.* **1991**, *56*, 1682-1684. doi:10.1111/j.1365-2621.1991.tb08670.x

26. Jankowska, R. Pankiewicz, K. Pogorzelec-Glaser, P. Ławniczak, A. Łapiński, J. Tritt-Goc, Comparison of structural, thermal and proton conductivity properties of micro- and nanocelluloses, *Carbohydr. Polym.* **2018**, *200*, 536-542. doi:0.1016/j.carbpol.2018.08.033
27. Prathapana, R. Thapa, G. Garnier, R. F. Tabor, Modulating the zeta potential of cellulose nanocrystals using salts and surfactants, *Colloids Surf. A Physicochem. Eng. Asp.* **2016**, *509*, 11-18. doi:10.1016/j.colsurfa.2016.08.075
28. Meneguzzo, C. Brunetti, A. Fidalgo, R. Ciriminna, R. Delisi, L. Albanese, F. Zabini, A. Gori, L. Beatriz dos Santos Nascimento, A. De Carlo, F. Ferrini, L. M. Ilharco, M. Pagliaro, Real-scale integral valorization of waste orange peel via hydrodynamic cavitation, *Processes* **2019**, *7*, 581. doi:10.3390/pr7090581
29. Panda, S. Manickam, Cavitation technology - the future of greener extraction method: a review on the extraction of natural products and process intensification mechanism and perspectives, *Appl. Sci.* **2019**, *9*, 766. doi:10.3390/app9040766

Figures

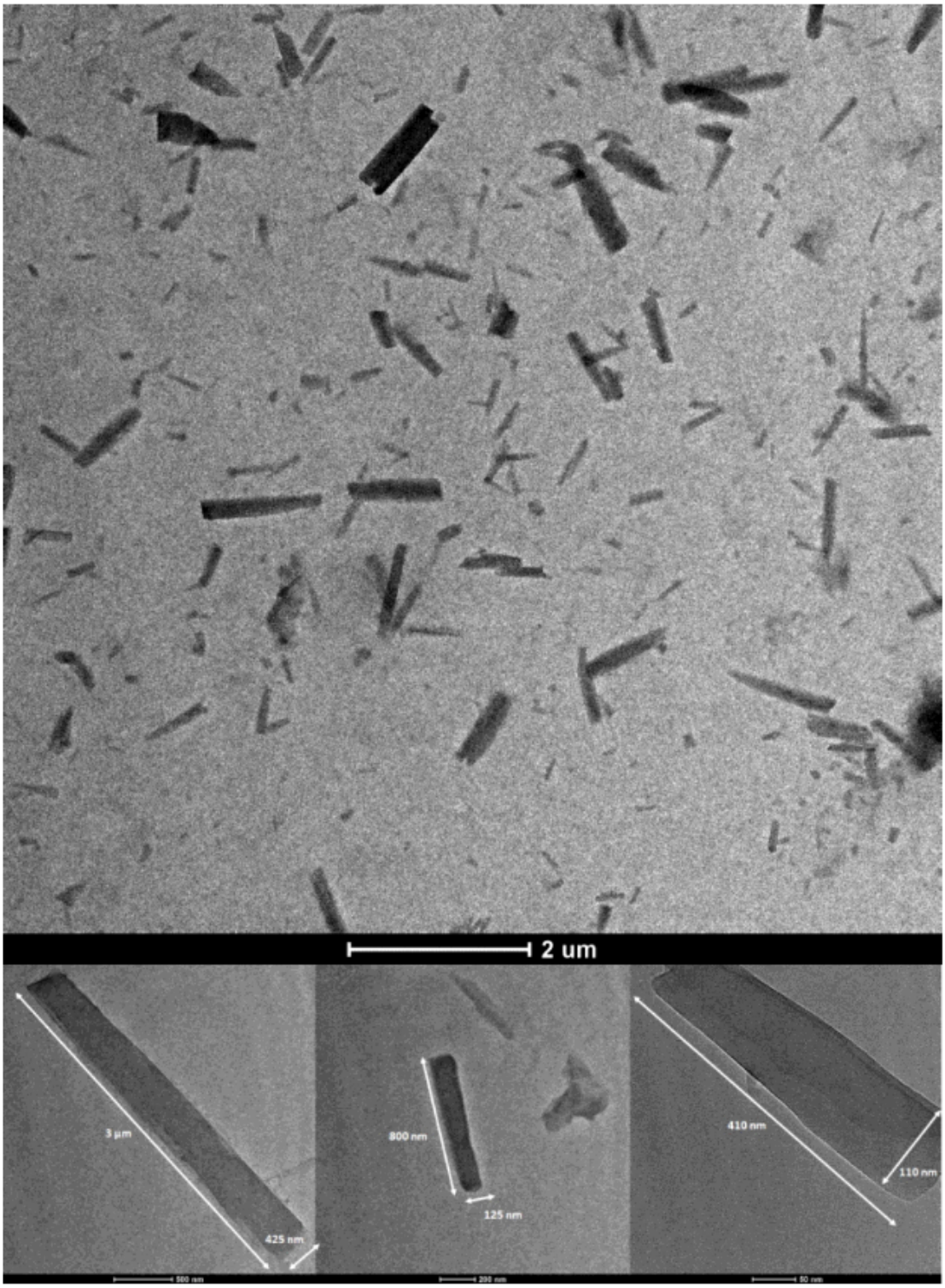

Figure 1

TEM images of lemon CytroCell (top) and after focusing on selected single fibrils (bottom).

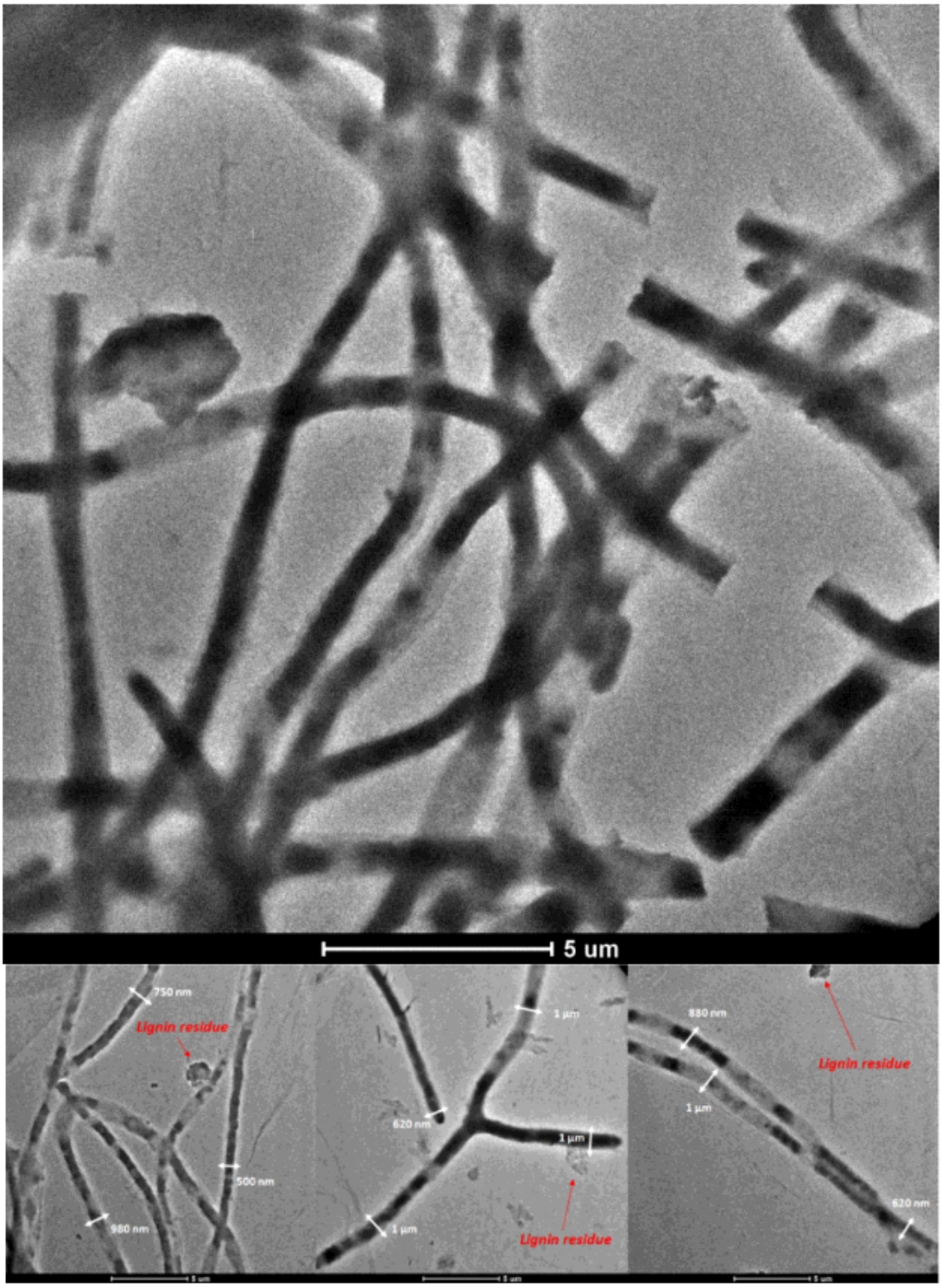

Figure 2

TEM images of grapefruit CytroCell (top) and after focusing on selected single fibrils (bottom).

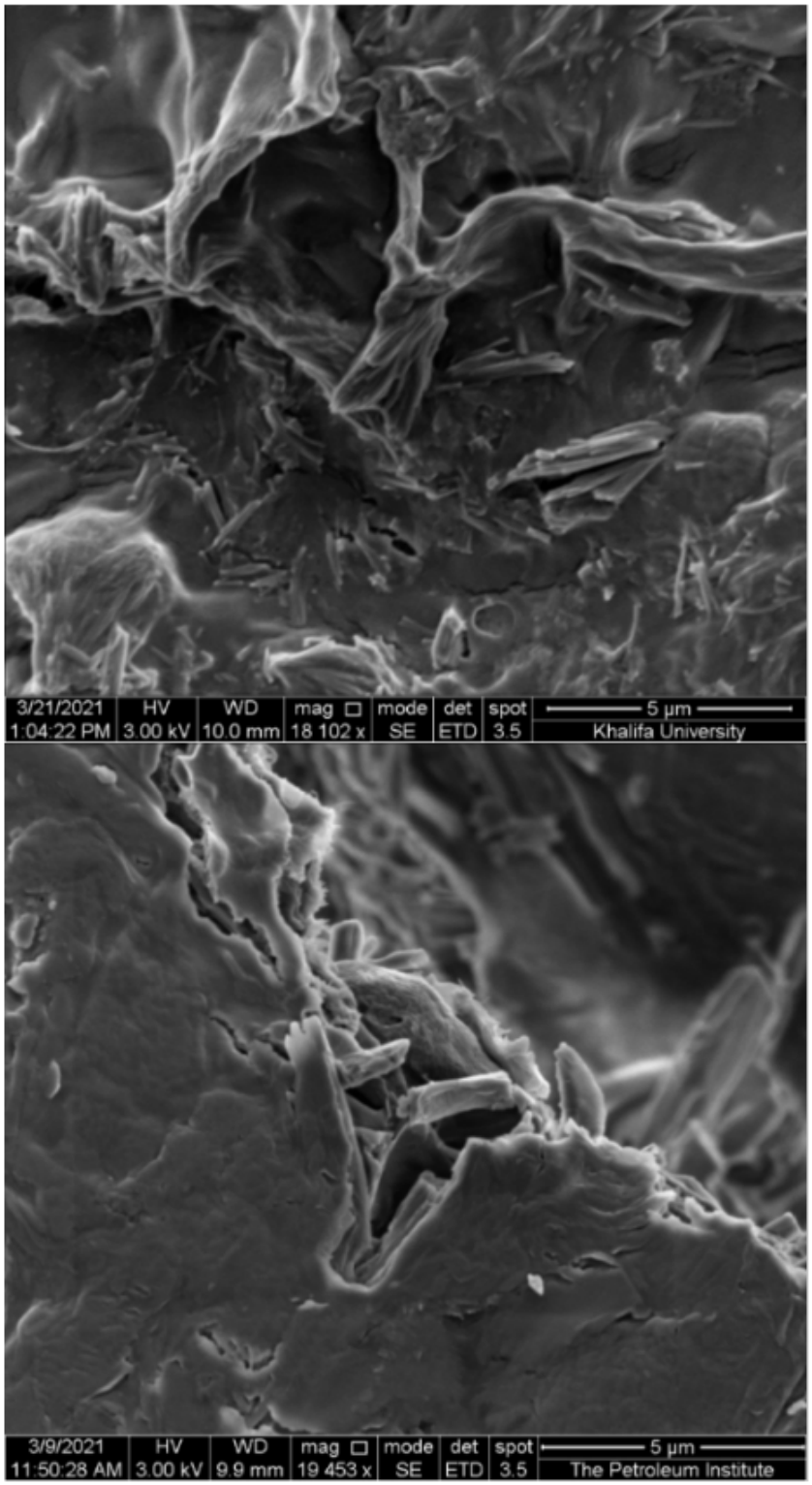

Figure 3

SEM images of lemon (top) and grapefruit (bottom) CytroCell.

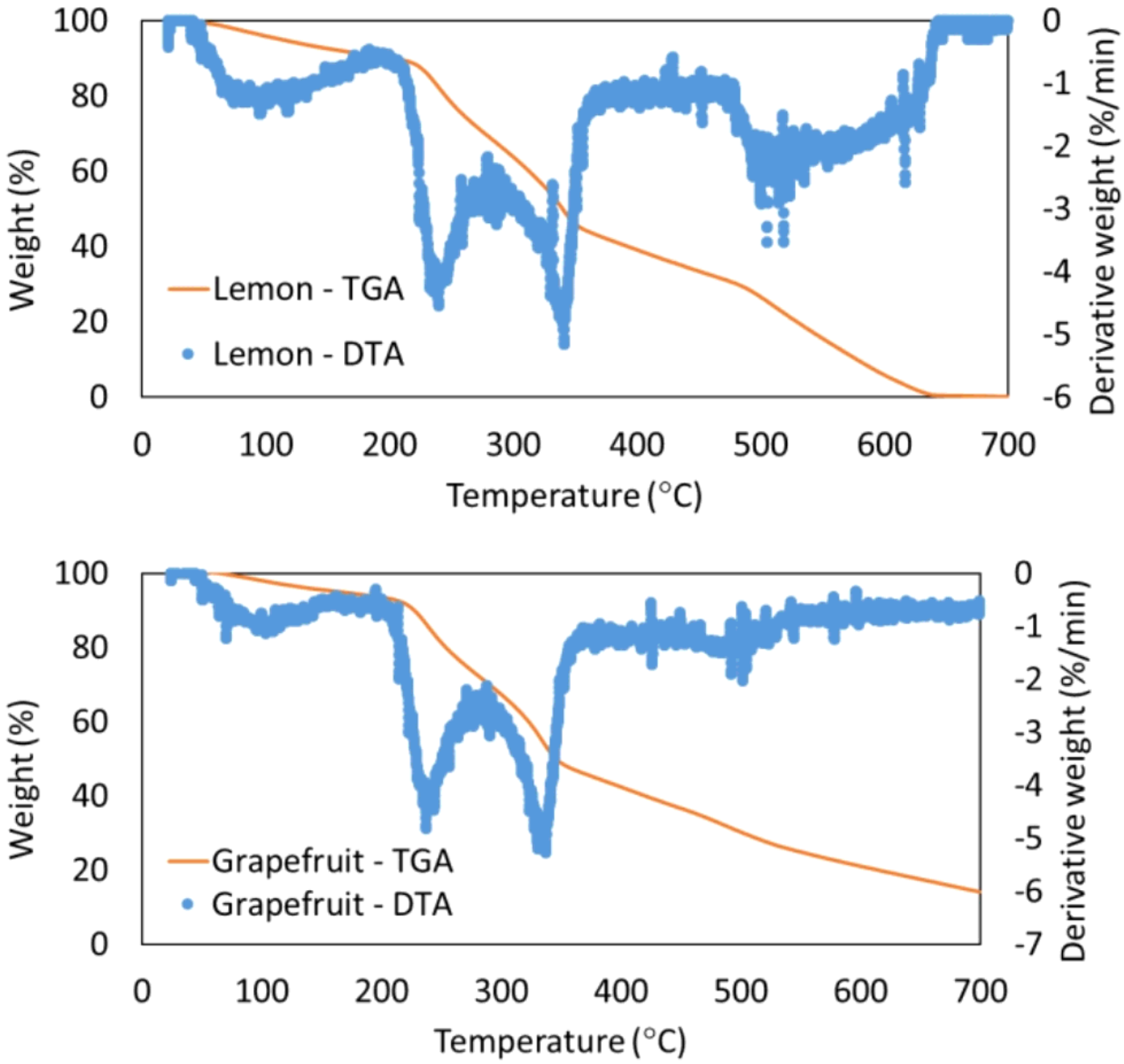

Figure 4

TGA and DTA curves for lemon (top) and grapefruit CytroCell (bottom).

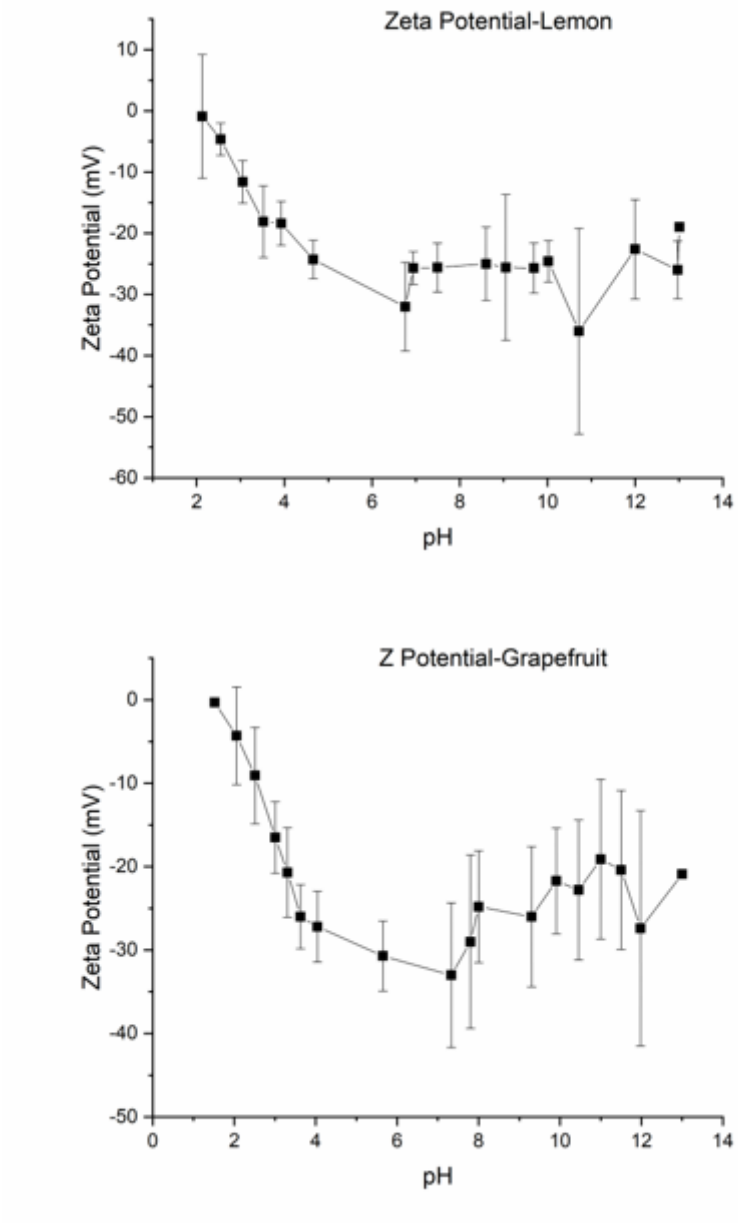

Figure 5

Zeta potential values at different pH for lemon (top) and grapefruit (bottom) CytroCell aqueous suspensions.